

Elastic electron scattering from formic acid (HCOOH): absolute differential cross-sections

V Vizcaino, M Jelisavcic, J P Sullivan and S J Buckman¹

Centre for Antimatter-Matter Studies, Atomic and Molecular Physics Laboratories, Research School of Physical Sciences and Engineering, Australian National University, Canberra, Australia
E-mail: stephen.buckman@anu.edu.au

New Journal of Physics **8** (2006) 85

Received 22 March 2006

Published 5 June 2006

Online at <http://www.njp.org/>

doi:10.1088/1367-2630/8/6/085

Abstract. We report experimental results for electron scattering from formic acid (HCOOH). A set of differential cross-sections is provided for elastic scattering at incident electron energies from 1.8 to 50 eV. Integral and momentum transfer cross-sections have also been derived from these results. Our results are compared, where possible, with recent theoretical calculations.

Contents

1. Introduction	2
2. Experimental apparatus	3
3. Result and discussion	4
3.1. Elastic DCS	4
3.2. ICS and MTCS	7
3.3. Role of dimers	8
4. Conclusion	9
Acknowledgments	9
References	9

¹ Author to whom any correspondence should be addressed.

1. Introduction

Until relatively recently, it was the commonly held belief that ballistic, high-energy impacts were responsible for the bulk of the cell and tissue damage when ionizing radiation enters the body. It now appears that the high-energy ionizing radiation entering the body liberates many low (sub-ionization) energy electrons which in turn can attach to the numerous electronegative components of DNA (bases, sugars and water). Through the process of dissociative attachment, this either directly leads to single or double DNA strand breaks, or to the formation of free radicals, which then can chemically react with DNA to lead to strand breaking [1]. There have been tremendous breakthroughs in this area in recent years and our goal is to add to this experimental endeavour by providing accurate absolute cross-sections for a range of these important building blocks of DNA.

The present study is the starting point of our investigations concerning these low-energy electron–biomolecule collision processes. Indeed, formic acid (HCOOH), which is the simplest organic acid, is thought to play a key role in the formation of bigger biomolecules such as acetic acid and glycine. In addition, the formate group ($-\text{COOH}$), is a key component of more complex biomolecules, including several amino acids.

To date, the majority of experimental studies of this molecule involving electron impact have been of dissociative electron attachment (DEA) [2]–[4]. These studies reveal different resonances leading to the decomposition of formic acid into HCOO^- , OH^- , O^- and H^- . The main resonance is found at 1.25 eV [2, 3] or 1.4 eV [4] and is correlated with the formation of the formate anion (HCOO^-). Electron transmission spectroscopy experiments [5, 6] and total scattering cross-section measurements [7] reveal a resonant state at around 1.7–1.8 eV due to electron attachment into the π^* orbital of the molecule. According to the energy range, this negative ion π^* resonance is likely responsible for the decomposition of the molecule into the formate ion. Tronc *et al* [6] have also measured energy loss spectra for both the formic acid monomer and dimer. On the theoretical side, Gianturco and Lucchese [8] carried out calculations to locate resonant states for formic acid in the low-energy region and found two distinct resonances, a π^* at around 3 eV and another resonance at around 12 eV. They believe that this π^* resonance leads indirectly to the dissociation of the molecule through vibrational energy redistribution from the C = O bond to the dissociative O–H stretching mode. Recently, Rescigno *et al* [9], with a different theoretical approach, localized this negative ion π^* resonance at 1.9 eV with a width of 0.2 eV, at equilibrium geometries and for the elastic cross-section. They point out that direct dissociation of the π^* anion in planar geometry to produce the formate anion is a symmetry forbidden process and that a second anion state, connected to the π^* state through a conical intersection at non-planar geometries, is involved in the dissociation mechanism. To our knowledge, there are no absolute differential scattering measurements in the literature for formic acid.

At room temperature, the vapour above a liquid sample of formic acid is predominantly constituted of hydrogen bonded dimers, rather than monomer molecules. The degree of dimerization depends on temperature and pressure, and can be calculated using the apparent molecular weight of the gas, which has been measured and listed for various values of T and P by Coolidge [10]. Typically, the dissociation into monomers is favoured at higher temperature and lower pressure. Formic acid has two stable planar forms, the *cis* and *trans* conformers (see figure 1). For the *trans* form, the two hydrogen atoms are located on opposite sides of the molecule relative to the C–O bond, as shown in figure 1(a). The energy difference between the two conformers in the gas phase is 1365 cm^{-1} (0.169 eV) [11]. A Boltzmann calculation of the

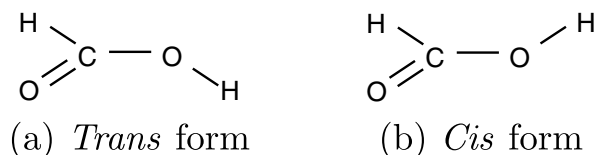


Figure 1. Formic acid molecule.

population ratio between the *trans* and the *cis* conformers indicates a clear predominance of the *trans* form at room temperature (~ 1000 times more abundant). Formic acid is also highly polar (1.41 Debye) and has a large dipole polarizability (~ 22.5 au). It thus poses considerable challenges for both experiment and quantum scattering theory.

In this paper, we present the first absolute differential elastic electron scattering cross-sections for formic acid. Angular differential cross-sections (DCS) are presented for eight incident electron energies between 1.8 and 50 eV. Our data are compared, where possible, with recent computations.

2. Experimental apparatus

Elastic electron scattering from formic acid has been studied using a crossed electron-target beam apparatus [12]. The formic acid, which has a purity greater than 98% (Sigma-Aldrich Australia; 27001), has been further purified by a number of freeze-pump-thaw cycles. It is admitted to the scattering system at a relatively low driving pressure via a temperature-controlled needle valve and gas-handling system. The needle valve and gas lines are set to a temperature of 70°C and the beam-forming capillary tube, through which the gas enters the collision region, is held at 130°C , at which temperature the beam is predominantly ($\sim 98\%$) composed of formic acid monomers. The low-energy electron beam is obtained from a conventional electron monochromator with reasonable energy resolution (FWHM around 60 meV) and scattered electrons are energy analysed before being detected by a channel electron multiplier.

The absolute value of the incident energy was determined through calibration against the positions of well-known resonances observed in electron-atom/molecule collision processes. For higher incident energies, we measured the position of the $1s\ 2s^2\ ^2S$ negative ion resonance feature for electron scattering from helium at 19.365 eV [13]. At lower energies, we used the $^2\Pi_g$ shape resonance features in N_2^- at around 2 eV [14].

Absolute cross-sections are determined using the relative flow technique [15]. This technique involves the measurements of relative electron scattering intensities for the gas under study (HCOOH) and for a so-called standard gas, in our case helium, for which there is an accurate set of DCS. The He cross-section established by Nesbet [16] is used as the absolute calibration for energies below 20 eV, and the tabulated cross-sections of Boesten and Tanaka [17] for higher energies. The driving pressures for both gases are determined in such a way that the collisional mean-free-path for both gases is the same in the region of the capillary. We could find no values of the hard sphere diameter for formic acid in the literature, so we have used molecular bond lengths to estimate its hard sphere diameter, from which the mean-free-path is calculated. Typical driving pressures used were 0.3 torr (HCOOH) and 0.9 torr (He).

Table 1. Absolute DCS for elastic scattering from formic acid, in units of $10^{-16} \text{ cm}^2 \text{ sr}^{-1}$. The uncertainty is given in parentheses (%). The integral elastic cross-section (ICS) and the momentum transfer cross-section (MTCS) for each incident energy are given in units of 10^{-16} cm^2 at the base of each column and the uncertainty on this value is estimated to be around 25%.

Angle	Incident energy (eV)							
	1.8	5	10	15	20	30	40	50
10	–	–	–	–	–	–	22.55 (8.3)	21.49 (9.1)
20	–	6.99 (26.4)	9.59 (25.6)	11.50 (9.2)	9.30 (15.7)	9.81 (8.7)	7.46 (14.3)	5.33 (7.6)
30	5.91 (17.1)	4.27 (13.1)	6.55 (16.4)	5.76 (8.5)	3.27 (20.4)	3.19 (12.2)	2.09 (9.9)	1.69 (8.9)
40	4.72 (16.9)	3.24 (10.9)	3.55 (10.9)	3.17 (9.4)	1.73 (17.3)	1.48 (11.8)	1.07 (11.4)	0.96 (9.1)
50	3.25 (8.3)	2.47 (9.8)	2.46 (10.5)	1.77 (11.4)	1.14 (12.6)	0.94 (9.2)	0.69 (13.9)	0.62 (7.6)
60	2.39 (8.6)	2.28 (8.3)	1.67 (8.1)	1.23 (7.3)	0.95 (12.8)	0.67 (8.9)	0.44 (8.3)	0.36 (12.7)
70	2.12 (8.8)	2.01 (7.3)	1.27 (7.9)	0.98 (7.8)	0.80 (9.3)	0.46 (9.8)	0.28 (12.4)	0.27 (15.9)
80	1.94 (8.1)	1.68 (7.6)	1.03 (8.2)	0.80 (7.4)	0.58 (13.8)	0.32 (13.2)	0.22 (11.6)	0.19 (9.9)
90	1.90 (7.3)	1.42 (8.9)	0.91 (9)	0.71 (7.8)	0.51 (12.6)	0.29 (11.2)	0.19 (11.7)	0.18 (10.7)
100	1.89 (7.6)	1.20 (7.8)	0.90 (10.2)	0.67 (7.9)	0.59 (13.5)	0.32 (16.8)	0.21 (10.7)	0.22 (9.4)
110	1.81 (7.4)	1.08 (8.6)	0.98 (11.3)	0.80 (7.6)	0.77 (15.2)	0.42 (13.5)	0.29 (15)	0.37 (9.1)
120	1.81 (8.4)	1.03 (8.6)	1.13 (11.7)	0.95 (7.3)	0.89 (14.5)	0.56 (19.6)	0.46 (12.1)	0.48 (17.7)
130	1.92 (9.2)	1.08 (9)	1.27 (11.3)	1.10 (7.6)	1.11 (12.5)	0.74 (18.1)	0.64 (13.8)	–
ICS	37.8	27.8	27.3	25.5	22.8	18.7	15.6	14.8
MTCS	16.3	15.6	16.3	14.6	16.8	10.8	8.75	9.2

The spectrometer can operate in two different data collection modes. In one, the angular dependence of the scattering signal is measured at fixed impact energy and energy loss, which leads to the measurement of angular DCS. In the other, we measure the energy dependence of the DCS at fixed energy loss and scattering angle. Details of these techniques are given in a previous paper [12]. The absolute uncertainties on the measured cross-sections vary between 7 and 25% but are typically less than 12%.

3. Result and discussion

3.1. Elastic DCS

Absolute DCS for elastic electron scattering from HCOOH are presented in table 1, and shown graphically in figures 2 and 3.

In figure 2, we compare the angular dependence of all of the DCS measurements. We see that the DCS does not change much in shape for energies between 10 and 50 eV, with a minimum at about 90° . However, the overall absolute magnitude of the DCS increases significantly with decreasing energy. At lower energies (1.8 eV), the DCS is essentially isotropic beyond a scattering angle of $\sim 60^\circ$.

In figure 3, we make a comparison, at a number of selected energies (1.8, 5, 10, 15, 30 and 50 eV), of the present results with the recent theoretical calculations of Gianturco and

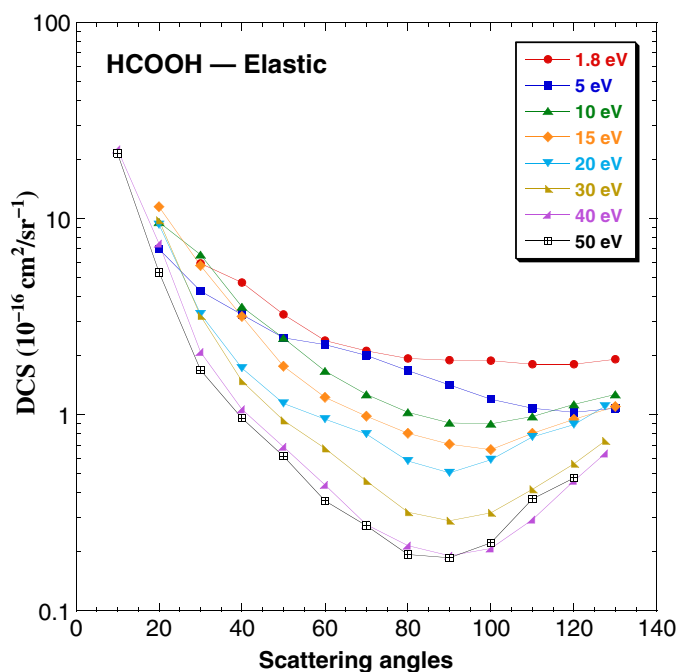


Figure 2. Absolute DCS for elastic electron scattering from HCOOH for incident energies between 1.8 and 50 eV.

Lucchese [18] and Trevisan *et al* [19], which have been carried out in both cases for the *trans* conformer. Trevisan *et al* performed fixed-nuclei calculations at equilibrium geometry using the complex Kohn variational method. The equilibrium nuclear positions were optimized at the self-consistent field (SCF) level. They determined the low order partial-wave components of the T-matrix variationally. Due to the polar nature of formic acid, they included the high order partial wave components of the T-matrix via a Born correction. Gianturco and Lucchese use a density functional approach within the fixed-nuclei approximation and include short-range correlation through the addition of a local, energy-independent potential. This potential is then corrected to agree with the long-range polarization effects. In general, the overall level of agreement between theory and experiment is quite good. At 1.8 eV (see figure 3(a)), the only direct comparison is with the calculation of Trevisan *et al* [19], which is about a factor of two higher than the experiment. However, in this region the cross-section magnitude is extremely sensitive to energy, as it is the region of the π^* resonance, and fixed nuclei calculations often lead to resonant cross-sections which are larger than experiment. Gianturco and Lucchese find the π^* resonance at an energy of 3.7 eV. At 5, 10 and 15 eV (see figures 3(b)–(d)), both theories follow the experimental data closely, especially at forward angles. At backward angles, the agreement with the computed values from Trevisan *et al* [19] is better. The calculation of Gianturco and Lucchese is lower than experiment at backward angles, and this difference becomes gradually larger as the energy increases (see figures 3(e) and (f)), while at forward angles the agreement is still good. According to Gianturco and Lucchese, this difference in the cross-section magnitude is probably due to their model treatment of the correlation–polarization forces.

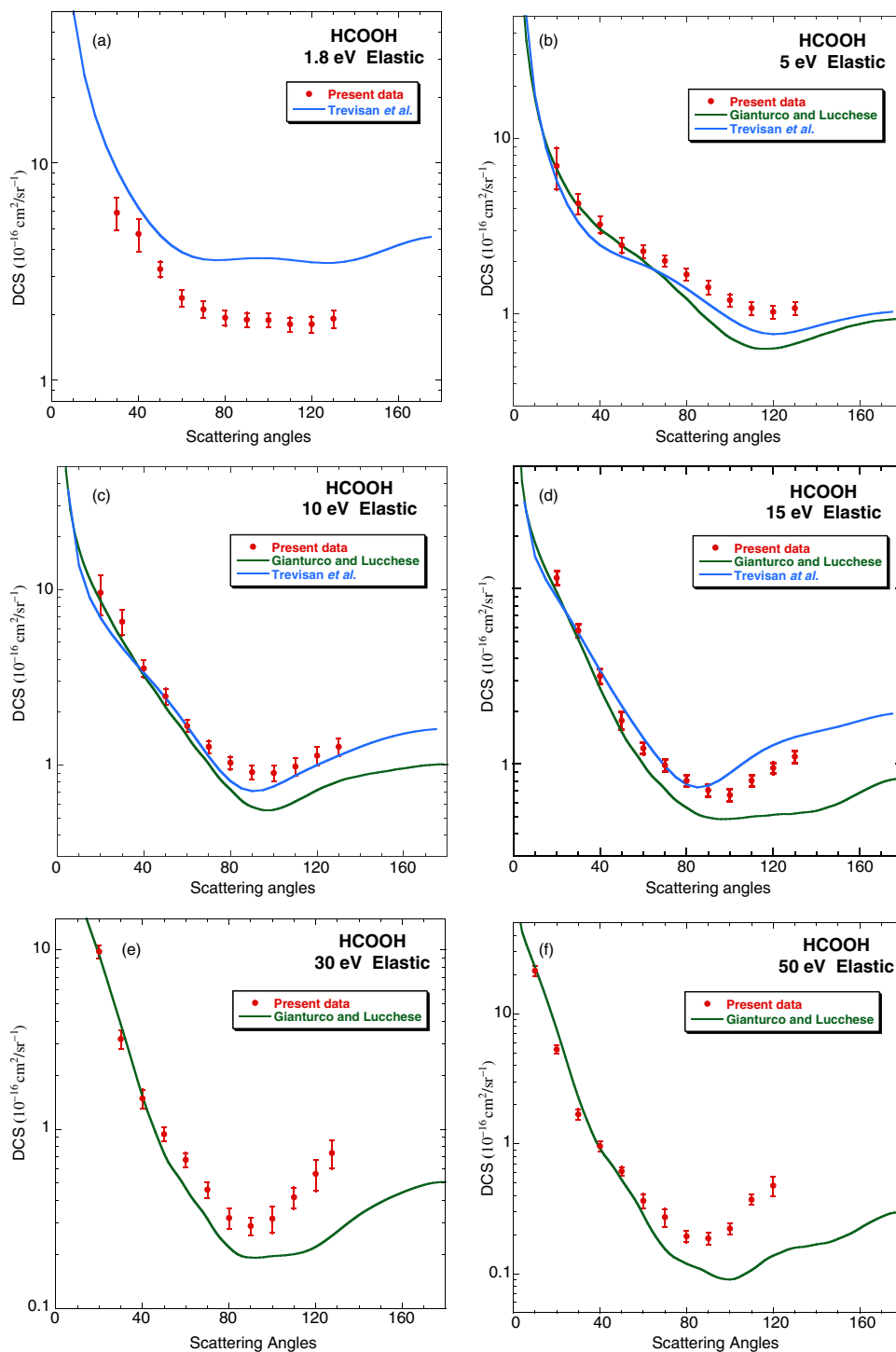


Figure 3. Absolute DCS for elastic electron scattering from HCOOH at: (a) 1.8 eV, (b) 5 eV, (c) 10 eV, (d) 15 eV, (e) 30 eV, (f) 50 eV. The experimental measurements are shown as (red ●) and the calculations for the *trans* conformer from Gianturco and Lucchese (green —) and from Trevisan *et al.* (blue —) are also shown where available.

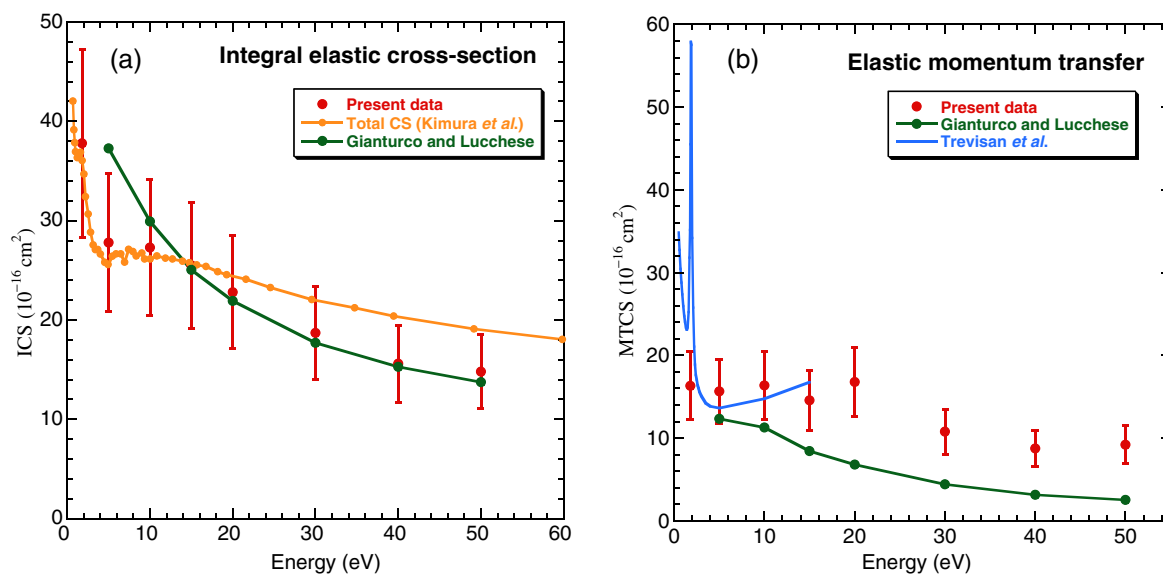


Figure 4. (a) ICS and (b) MTCS for elastic electron scattering from HCOOH. The present result (red ●), the total cross-section from Kimura *et al* (orange ●), the Gianturco and Lucchese (green —) and the Trevisan *et al* (blue —) calculations are shown.

3.2. ICS and MTCS

The DCS have been extrapolated to both forward and backward angles in order to calculate the ICS and the elastic MTCS for each of the eight incident energies. For a strongly polar molecule such as formic acid, the extrapolation to forward angles is a highly uncertain process. As the agreement between the present DCS measurements and the theoretical calculations is quite good, we have used the theoretical values of Gianturco and Lucchese as a guide for the extrapolation process. The integral and momentum transfer cross-section values are given in table 1 at the foot of each column. The uncertainty of these values, mainly due to the extrapolation, could be as large as 30%.

In figure 4, we make a comparison between the values derived from the present DCS measurement and the computed values from Gianturco and Lucchese [18] and from Trevisan *et al* [19] for the monomer (*trans* conformer). The discrepancies between theory and experiment which were seen at the DCS level are reflected here. Indeed, in the region of the π^* resonance, the MTCS is more than 3 times smaller than the calculated values of Trevisan *et al*. At higher energies, the experimental cross-section is appreciably higher than the computed values of Gianturco and Lucchese for both the ICS and MTCS, due largely to the discrepancies in the DCS at backward angles.

In figure 4(a), we also compare our present result with the total scattering cross-section measured by Kimura *et al* [7] and there is a broad overlap, within the experimental error bars. This comparison would appear to indicate that inelastic scattering (vibrational, electronic, dissociation and ionization) is apparently quite small or negligent. This is unlikely, and further studies of inelastic scattering should be able to shed further light on this issue.

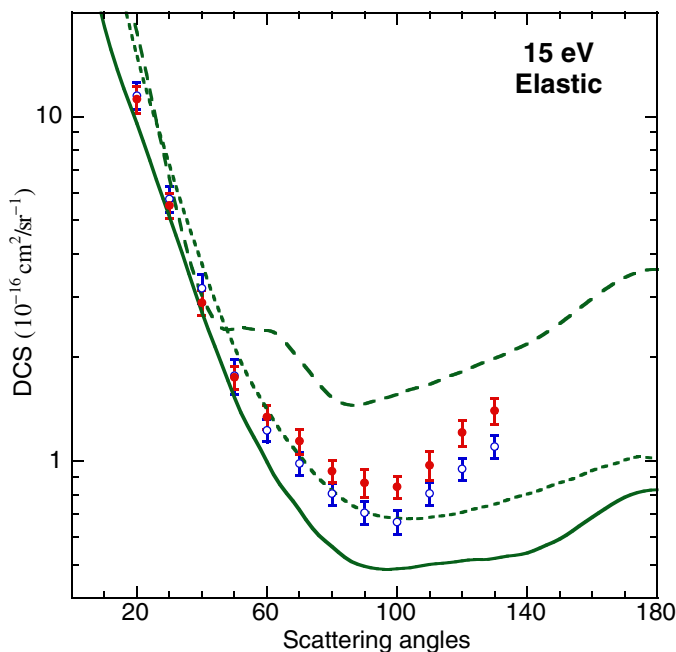


Figure 5. Absolute DCS for elastic electron scattering from HCOOH for an incident energy of 15 eV. The experimental measurements are shown at room temperature (\bullet) and elevated temperature (\circ). The Gianturco and Lucchese calculations for *trans* (—), *cis* ($\cdots\cdots$) and dimers (- - -) are also shown.

3.3. Role of dimers

At room temperature, and for a driving pressure of 0.3 torr, the formic acid beam is estimated to contain around 20% of dimers. By operating the apparatus (gas lines and the beam-forming capillary tube) at room temperature, the influence of dimers on the DCS magnitude can be shown. In figure 5, we compare the values of DCS measurements for an incident energy of 15 eV for both room and high-temperature operation. At room temperature, DCS is similar at forward angles to the high-temperature (monomer) measurement, but somewhat higher at backward angles. Using the calculations of Gianturco and Lucchese as a guide, they indicate a similar DCS magnitude for the dimer at forward scattering angles, but a much larger dimer cross-section beyond about 60° . Thus the trend in the experimental cross-section as a function of temperature is largely consistent with theory. In principle, we could estimate the absolute DCS for the dimer from these data but in practice it would be highly uncertain. Indeed, although the gas lines and capillary were operated at room temperature, the experiment was performed with the needle valve still at $\sim 70^\circ\text{C}$, to enable stable flow. As a result, it is difficult to estimate the absolute DCS, as measured flow rates for the dimer could not be used. Future plans involve measurements with the whole system at room temperature which may enable a more accurate estimate of the flow rates for a mixed dimer/monomer beam.

4. Conclusion

The present paper provides the first set of absolute DCS for elastic electron scattering from formic acid. Data at energies between 1.8 and 50 eV are in reasonably good agreement with the recent theoretical calculations of Trevisan *et al* and Gianturco and Lucchese. Measurements of vibrational excitation, and the role of resonant scattering, are presently under way.

Acknowledgments

It is a pleasure to acknowledge discussions with Robert Lucchese, Franco Gianturco, Cynthia Trevisan, Tom Rescigno and Anne Orel and to thank all of them for the provision of tabulated data prior to publication. Violaine Vizcaino acknowledges support from the Australian National University and Flinders University.

References

- [1] Boudaiffa B, Cloutier P, Hunting D, Huels MA and Sanche L 2000 *Science* **287** 1658
- [2] Pelc A, Sailer A, Scheier P, Probst M, Mason N J, Illenberger E and Mark T D 2002 *Chem. Phys. Lett.* **361** 277–84
- [3] Pelc A, Sailer A, Scheier P, Mason N J, Illenberger E and Mark T D 2003 *Vacuum* **70** 429
- [4] Prabhudesai V S, Nandi D, Kelkar A H, Parajuli R and Krishnakumar E 2005 *Chem. Phys. Lett.* **405** 172
- [5] Aflatooni K, Hitt B, Gallup G A and Burrow P D 2001 *J. Chem. Phys.* **115** 6489
- [6] Tronc M, Allan M and Edard F 1987 *Abstract of Contributed Papers, XVth ICPEAC, Brighton* p 335
- [7] Kimura M, Sueoka O, Hamada A and Itikawa Y 2004 *Adv. Chem. Phys.* **III** 537
- [8] Gianturco F A and Lucchese R R 2004 *New J. Phys.* **6** 66
- [9] Rescigno T N, Trevisan C S and Orel A E 2006 *Phys. Rev. Lett.* submitted
- [10] Coolidge A S 1928 *J. Am. Chem. Soc.* **50** 2166
- [11] Hocking W H 1976 *Z. Naturforsch. A* **31** 1113
- [12] Gibson J C, Morgan L A, Gulley R J, Brunger M J, Bundschu C T and Buckman S J 1996 *J. Phys. B: At. Mol. Opt. Phys.* **29** 3197
- [13] Gopalan A, Bommels J, Gotte B, Landwehr A, Franz K, Ruf M W, Hotop H and Bartschat K 2003 *Eur. Phys. J. D* **22** 1729
- [14] Rohr K 1977 *J. Phys. B: At. Mol. Opt. Phys.* **10** 2215
- [15] Brunger M J and Buckman S J 2002 *Phys. Rep.* **357** 215
- [16] Nesbet R K 1979 *Phys. Rev. A* **20** 58
- [17] Boesten L and Tanaka H 1992 *At. Data Nucl. Data Tables* **52** 25
- [18] Gianturco F A and Lucchese R R 2006 private communication
- [19] Trevisan C S, Orel A E and Rescigno T N 2006 *Phys. Rev. A* submitted